IOP Conference Series: Materials Science and Engineering

**PAPER** • **OPEN ACCESS**

# Research on the Vapor Injection of Two-stage Rotary Compressor

To cite this article: Y S Hu *et al* 2019 *IOP Conf. Ser.: Mater. Sci. Eng.* **604** 012072

IOP Conf. Series: Materials Science and Engineering **604** (2019) 012072 doi:10.1088/1757-899X/604/1/012072

# Research on the Vapor Injection of Two-stage Rotary Compressor

**Y S Hu[1, 2], H J Wei[1,2], B Yu[1, 2], O X Yang[2], J Wang[2] and J Wu[2]**
[1] State Key Laboratory of Air-conditioning Equipment and System Energy Conservation, ZhuHai, Guangdong 519070, China
Phone: +86-756-8589881, Fax: +86-756-8668386
E-mail: jvcanjian@163.com
[2] Gree Electric Appliances, Inc. of Zhuhai, ZhuHai, Guangdong 519070, China

**Abstract.** In order to understand the vapor injection flow characteristics of two-stage rotary compressor in the course of compression, a mathematical model based on mass conservation equation, energy equation and thermodynamic identity was established and proved by P-V diagram testing results. Some useful conclusions about pressure in the intermediate chamber and mass flow of vapor injection in the course of compression were also given out. The results show that, gas backflow between the intermediate chamber and the vapor injection channel is an important defection of two-stage rotary compressor which can be solved by the application of injection valve in vapor injection channel. The injection valve can obviously reduce the gas backflow and the power loss in the course of compression while increasing the pressure fluctuation in the intermediate chamber. Experiments show that the COP of two-stage rotary compressor with the injection valve increased by over 2% in ASHRAE/T working condition.

## 1. Introduction

The two-stage rotary compressor can overcome the shortcomings of heating capability reduction, poor reliability and low efficiency of single-stage compressor in low temperature environment [1]. Therefore, it has been studied and applied in air source heat pump air conditioners, heat pump water heaters and heating machines, especially in the cold regions of the world [2-4].

Vapor injection parameters are the key factors affecting the efficiency of the two-stage compression system. Jin X and Jiang S et al. studied the fluctuation characteristics of intermediate pressure and its influence on the performance, analyzed the effects of subcooling parameters and the respective efficiencies of two compressors on the intermediate pressure, and proposed a volume-ratio selection method based on weather data [5-7]. Xu S X et al. investigated the influence of vapor injection parameters on the relative injection mass, COP and exhaust temperature [8-9]. Redón A et al. analyzed the design parameters (such as displacement ratio) and injection conditions of two-stage cycles with four refrigerants [10]. The related researches haven't studied the course of vapor injection in the single-machine two-stage rotary compressor, so it is impossible to guide the efficient design of the intermediate chamber and the injection structure. In this paper, the flow characteristics of the injection vapor are analyzed by numerical and experimental methods.

## 2. Mathematical model

Figure 1 shows the single-machine two-stage rotary compressor and its system cycle [11-12]. Figure 2 shows the *p-h* diagram of the two-stage expansion cycle with flash tank.

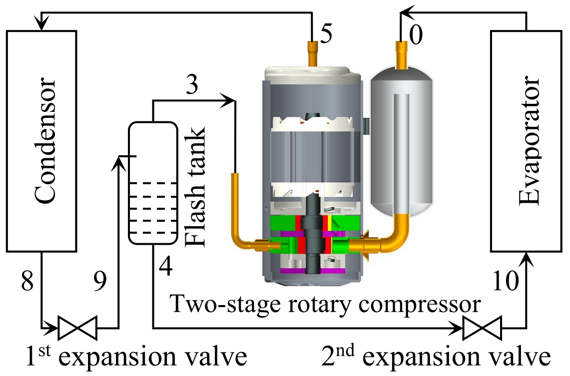


**Figure 1.** The two-stage compression system

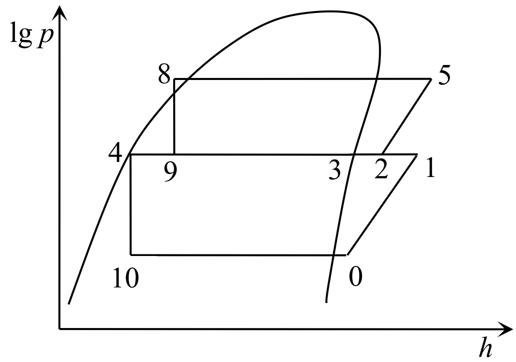


**Figure 2.** *p-h* diagram of the system

The geometry, leakage and heat transfer models of rotary compressor are well known [13-14]. Therefore, only the intermediate chamber model and the injection channel model are explained below.

### *2.1 Model of the intermediate chamber*

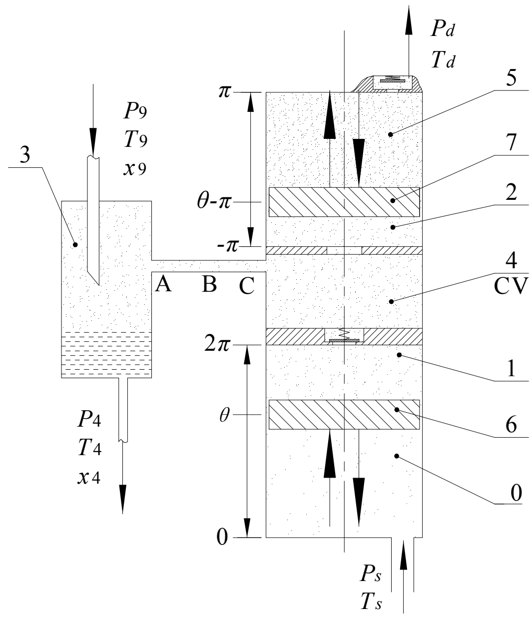


0- Suction chamber of the first stage cylinder
1- Compression chamber of the first stage cylinder
2- Suction chamber of the second stage cylinder
3- Flash tank
4 (CV) - Intermediate chamber
5- Compression chamber of the second stage cylinder
A- Injection channel inlet
B- Injection channel
C- Injection channel outlet
6- First stage rolling piston
7- Second stage rolling piston

**Figure 3.** Two-stage rotary compression mechanism and vapor injection structure

As shown in Figure 3, each rolling piston divides each cylinder working chamber into a suction chamber and a compression chamber. When the 1st stage crank angle is $\theta$ ($0\leq\theta\leq2\pi$), the 2nd stage crank angle is $\theta$-π ($-\pi\leq\theta-\pi\leq\pi$). The intermediate chamber is located between the 1st stage cylinder exhaust valve and the 2nd stage cylinder suction port, and communicates with the flash tank through the injection channels ABC. So, its thermodynamic parameters are affected by the thermodynamic state and flow state of the inlet (the first stage cylinder exhaust), the outlet (the second stage cylinder suction), and the variable port (the injection channel). Therefore, it belongs to a variable mass system. The following assumptions are made: (a) The refrigerant is evenly distributed in the chamber, and the state parameters are uniform; (b) The variations of the potential energy and kinetic energy are ignored. The intermediate chamber is used as the control volume (CV). The energy equation, mass conservation equation and thermodynamic identity [15] are expressed as:

$$\frac{\mathrm{d}E_{CV}}{\mathrm{d}\theta}=\frac{\mathrm{d}Q}{\mathrm{d}\theta}+h_1\frac{\mathrm{d}m_1}{\mathrm{d}\theta}-h_2\frac{\mathrm{d}m_2}{\mathrm{d}\theta}+(-1)^n h_C\frac{\mathrm{d}m_C}{\mathrm{d}\theta} \tag{1}$$

$$\frac{\mathrm{d}m_4}{\mathrm{d}\theta}=\frac{\mathrm{d}m_1}{\mathrm{d}\theta}-\frac{\mathrm{d}m_2}{\mathrm{d}\theta}+(-1)^n\frac{\mathrm{d}m_C}{\mathrm{d}\theta} \tag{2}$$

$$\mathrm{d}u=c_V\mathrm{d}T+\left[T\left(\frac{\partial p}{\partial T}\right)_v-p\right]\mathrm{d}v \tag{3}$$

The volume of the intermediate chamber is unchanged, then

$$\mathrm{d}v=\frac{V_4}{m_4+\mathrm{d}m_4}-\frac{V_4}{m_4} \tag{4}$$

Substituting equations (3) and (4) into equation (1):

$$\frac{\mathrm{d}T_4}{\mathrm{d}\theta}=\frac{1}{m_4c_V}\left\{h_1\frac{\mathrm{d}m_1}{\mathrm{d}\theta}-h_2\frac{\mathrm{d}m_2}{\mathrm{d}\theta}+(-1)^n h_C\frac{\mathrm{d}m_C}{\mathrm{d}\theta}+\frac{\mathrm{d}Q}{\mathrm{d}\theta}-\left\{u_4-\left[T_4\left(\frac{\partial p}{\partial T}\right)_v-p_4\right]\frac{V_4}{m_4+\mathrm{d}m_4}\right\}\frac{\mathrm{d}m_4}{\mathrm{d}\theta}\right\} \tag{5}$$

Where, $E_{CV}$ is the total energy of control volume, $Q$ is the heat exchange capacity between the control volume and its wall, $h$ is the enthalpy, $u$ is the thermodynamic energy, $c_V$ is the heat capacity at constant volume, $v$ is the specific volume, $p$ is the refrigerant pressure, $\rho$ is the refrigerant density, T is the temperature, and $\theta$ is the crankshaft angle. When $p_3>p_4$, the gas in the flash tank flows into the control volume, then $n$=2. When $p_3<p_4$, the gas in the control volume flows into the flash tank, then $n$=1. The heat exchange capacity $Q$ is calculated based on the average Nusselt number $Nu$ of the Sieder-Tate equation [16].

### *2.2 Model of the injection channel*

The gas in the flash tank is saturated vapor under the injection pressure ($p_3$), and its state parameters are determined by the working condition. Because both the flash tank and the control volume are filled with refrigerants in a certain pressure, the flow is regarded as submerged outflow. As shown in Figure 3, the injection channel is divided into three sections, which are the injection channel inlet A, the injection channel B and the injection channel outlet C.

Considering that the gas mass flow is not high and the pressure variation is slow, the flow in the injection channel is assumed as follows: (a) Quasi-stationary adiabatic flow. (b) The gas in the pipe can be compressed. (c) The potential energy of the refrigerant is ignored. (d) The heat exchange is ignored. The governing equation for pipe flow is as follows [17].

**Table 1.** Mathematical model of the vapor injection flow

| Position | Equation | Expression |
|---|---|---|
| Inlet A | Energy equation | $p_3 + 0.5\alpha_3\rho_3 c_{f3}^2 = p_A + 0.5\alpha_A\rho_A c_{fA}^2 + 0.5\xi_A\rho_A c_{fA}^2$ |
| | Mass equation | $S_3\rho_3 c_{f3} = S_A\rho_A c_{fA}$ |
| Channel B | Mass equation | $\frac{\mathrm{d}\rho}{\rho} + \frac{\mathrm{d}c_f}{c_f} = 0$ |
| | Momentum equation | $\mathrm{d}p + \frac{\lambda\rho c_f^2\mathrm{d}x}{2d} + \rho c_f\mathrm{d}c_f = 0$ |
| | Energy equation | $c_P\mathrm{d}T + c_f\mathrm{d}c_f = 0$ |
| | Adiabatic equation | $\frac{\mathrm{d}p}{p} - \kappa\frac{\mathrm{d}\rho}{\rho} = 0$ |
| Outlet C | Energy equation | $p_4 + 0.5\alpha_4\rho_4 c_{f4}^2 = p_C + 0.5\alpha_C\rho_C c_{fC}^2 + 0.5\xi_C\rho_C c_{fC}^2$ |
| | mass equation | $S_C\rho_C c_C = S_4\rho_4 c_{f4}$ |

Where, $c_f$ is the flow speed of refrigerant, $\lambda$ is the resistance factor of the injection channel, $\alpha$ is the kinetic energy correction factor, $\zeta$ is the local loss coefficient, $c_p$ is the heat capacity at constant pressure, $d$ is the diameter of the injection channel B, and $S$ is the cross-sectional area of flow.

*2.3 Program*

A simulation program of the course of vapor injection is established by using the software MATLAB. The flow chart of calculation program is presented in Figure 4.

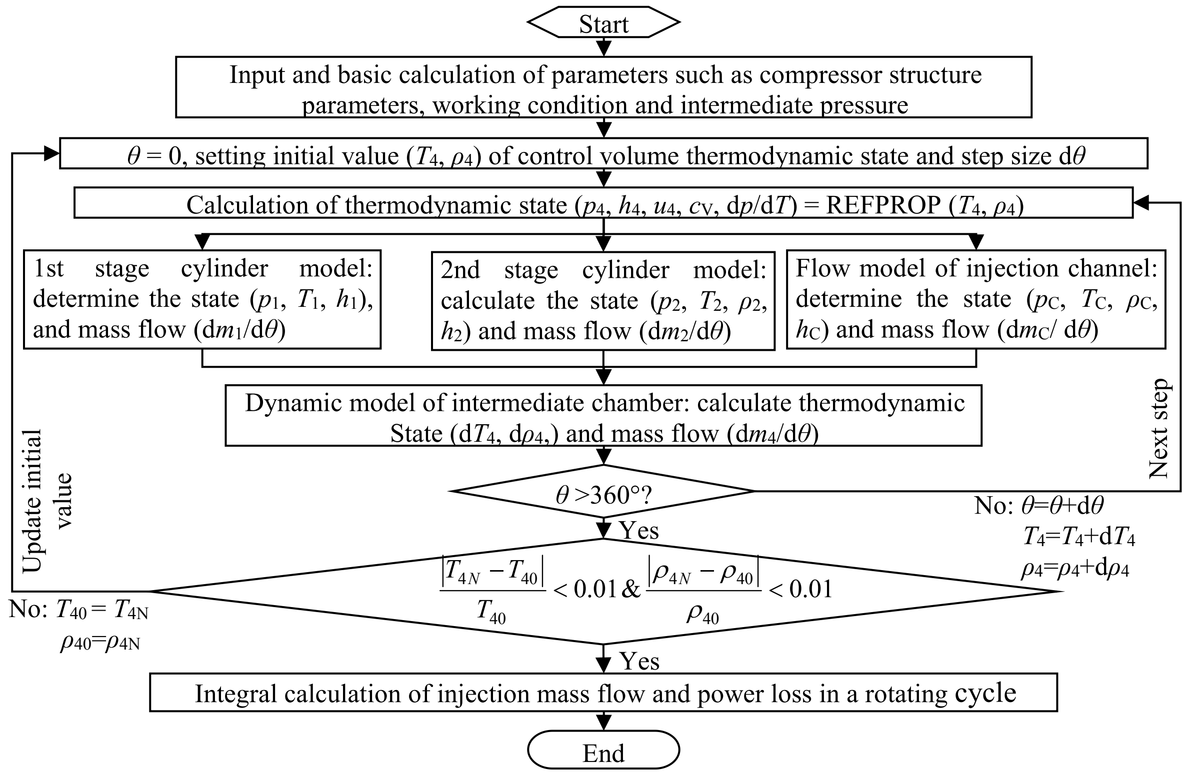


Figure 4. Flow chart of calculation program

IOP Conf. Series: Materials Science and Engineering **604** (2019) 012072 doi:10.1088/1757-899X/604/1/012072

The thermodynamic parameters of R410A are calculated by the software REFPROP. The refrigerant parameters in the intermediate chamber, the mass flow and energy exchange of the vapor injection are calculated at each small angle step with the crankshaft rotating for one cycle. So, the flow characteristics in the course of vapor injection can be studied.

## 3. Model validation

A P-V prototype was made to measure the pressure at different working chambers. Figure 5 shows the measuring point distribution and Figure 6 shows the P-V test system. The flange marking the angle of crankshaft is set at the top of the crankshaft, and the crankshaft angle is measured by the displacement sensor. By means of the above method, the variation of pressure with crankshaft angle can be measured. The P-V prototype is connected to the compressor refrigeration capacity test bench for testing. The cycle diagram of the test system has been given in the literature [18]. The analysis method of experimental data is the same as reference [19].

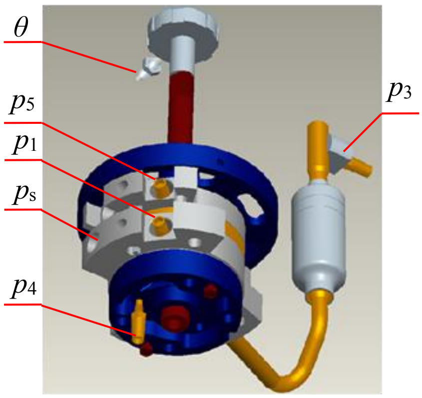


**Figure 5.** Measuring point distribution

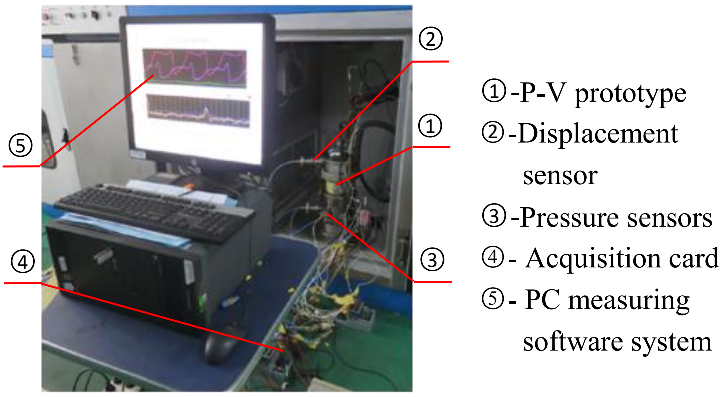


**Figure 6.** P-V test system

Taking the single-machine two-stage rotary compressor produced by GREE Electrical Appliances Co., Ltd. as an example, the flow characteristic of vapor injection under ASHRAE/T condition was simulated and measured. When testing the compressor with a flash tank, it is necessary to set the injection pressure ($p_3$) at the same time, in addition to the parameters specified in the working condition. Figure 7 shows Experimental verification when $p_3$=1750kPa.

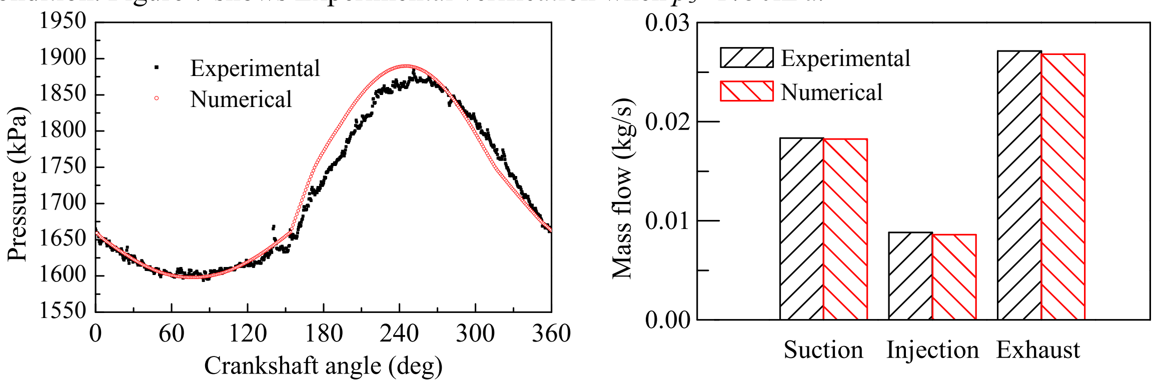


(a) Pressure in the intermediate chamber ($p_4$) (b) Mass flow

**Figure 7.** Experimental verification for vapor injection of two-stage rotary compressor

From figure 7-(a), it can be seen that the simulated values of pressure in the intermediate chamber ($p_4$) are in good agreement with the measured values of P-V test. The maximum deviation between the simulated and experimental values is less than 3% under different crankshaft angles. From figure 7-(b), the calculation errors of mass flow of suction, injection and exhaust are all within 2.7%.

Furthermore, $p_4$ has a pulsating characteristic, and the peak-valley difference reaches 290 kPa, reaching 17% of the time-average value. The reasons are analyzed as follows. (a) The exhaust of the 1st stage cylinder has pulse characteristics. When the 1st stage cylinder exhaust valve is opened and refrigerant is forced into intermediate chamber, the pressure rises rapidly. As shown in Figure 7-(a), the inflection point where the pressure begins to rise rapidly appears at the exhaust angle of 156 degree. (b) Although the suction of the 2nd stage cylinder is continuous, the variation rate of the suction volume has pulse characteristics. The difference of crankshaft angles between two cylinders is 180°. When the exhaust speed of the 1st stage cylinder is fast, the suction speed of the second cylinder is slow. When the 1st stage cylinder does not exhaust or the exhaust speed is slow, the suction speed of the 2nd stage cylinder is fast.

Therefore, the rate of mass exchange between the two cylinders and the intermediate chamber is very mismatched, resulting in significant fluctuation of pressure in the intermediate chamber.

## 4. Simulation results & Discussions

### *4.1 Effect of intermediate chamber volume on vapor injection characteristic*

The working volume of the 1st stage cylinder is $V_1$, and the volume of intermediate chamber $V_4$ is set to be 1, 2, 3 and 5 times $V1$ respectively. The variations of $p_4$ and the vapor injection mass flow $\dot{m}_C$ are simulated as $p_3$=1750kPa.

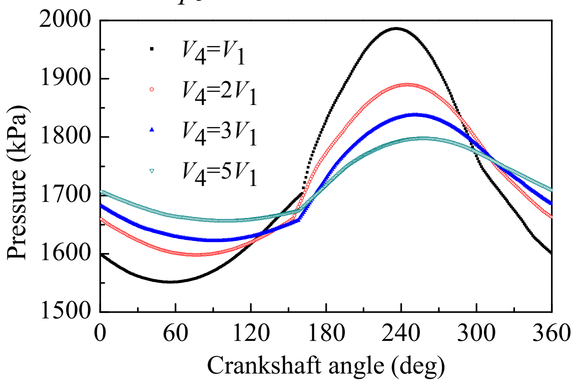


**Figure 8.** The variety of $p_4$

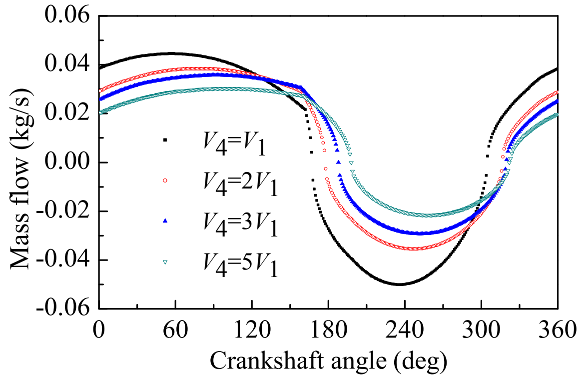


**Figure 9.** The variety of $\dot{m}_C$

From Figure 8, the peak-valley difference of pressure fluctuation decreases continuously with the increase of $V_4$. When $V_4 = 5V_1$, the peak-valley difference of $p_4$ is 141 kPa, which is only 32% of the difference for $V_4= V_1$. So, the pressure fluctuation amplitude can be effectively reduced by increasing the volume of the intermediate chamber and playing a buffer role. As can be seen from Figure 9, $\dot{m}_C$ have some positive and negative values, and the negative values represent that the vapor flows back from the intermediate chamber into the flash tank. The mass flow of the vapor backflow decreases with the increase of $V_4$.

*4.2 Effect of injection valve on vapor injection Characteristics*

In order to eliminate the phenomenon of vapor backflow in the intermediate chamber, an injection valve is installed at the outlet C of the vapor injection channel, and its effects on $p_4$ and $\dot{m}_C$ are compared by simulation as $p_3$=1750kPa.

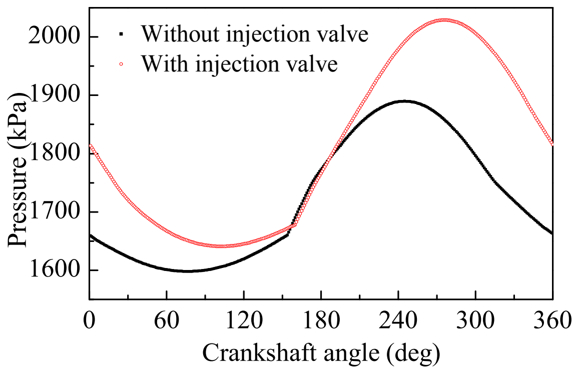


**Figure 10.** The variety of $p_4$

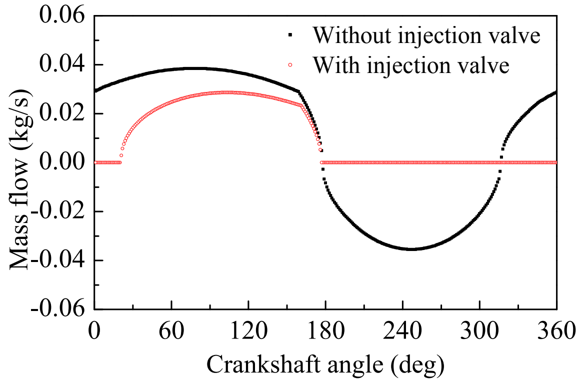


**Figure 11.** The variety of $\dot{m}_C$

From Figure 10, it can be seen that the pressure fluctuation of $p_4$ is increased by using injection valve, and the peak-valley difference is increased from 290 kPa to 388 kPa. The main reason is that the valve closes the vapor injection channel when the 1st cylinder exhausts, which is equivalent to closing the pressure relief channel of the intermediate chamber, so that the peak pressure is larger than the value without injection valve. From Figure 11, it can be seen that the forward mass flow with injection valve decreases, but the backflow of the vapor in the injection channel is avoided. The effective mass flow increases by 18%, and it is only 35% of the total mass flow of the forward and back flow without injection valve.

*4.3 Effect of injection valve on flow power loss of vapor injection*

Figure 12 shows the effect of injection valve on flow power loss of vapor injection. The flow power loss without injection valve is defined as 100% when $V_4 = V_1$.

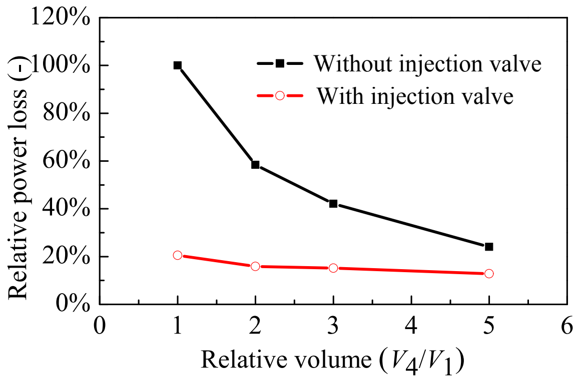


**Figure 12.** The flow power loss of vapor injection

The flow power loss without injection valve decreases fast with the increase of $V_4$, but the variation of $V_4$ has little effect on the power loss with injection valve. The flow power loss with injection valve is significantly lower than that without injection valve, for example, the power loss decreases by 72% when $V_4 = 2V_1$. The reason is that the pressure loss caused by back flow is much larger than that caused by the injection valve. It can be seen that the back flow of the gas in the intermediate chamber without the injection valve leads to the increase of the flow power loss and the decrease of the

IOP Conf. Series: Materials Science and Engineering **604** (2019) 012072 doi:10.1088/1757-899X/604/1/012072

effective mass flow, which is an important factor affecting the performance of the two-stage rotary compressor.

## 5. Optimized prototype verification

Figure 13 shows an injection valve structure of the two-stage rotary compressor, which includes a reed valve and a baffle [20]. A demountable prototype was made, and different parts of the intermediate chamber were replaced to verify the effect of the injection valve on the actual performance of the compressor.

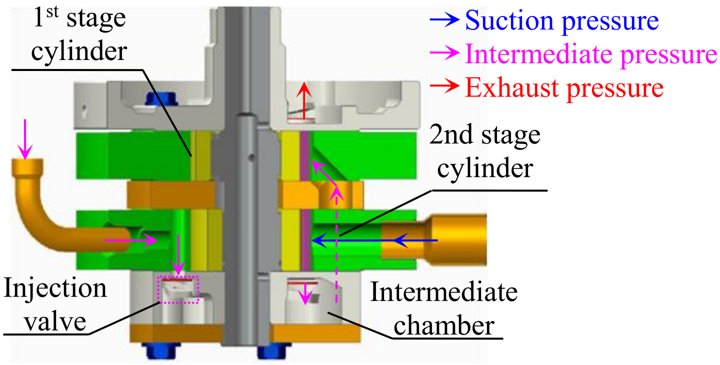


**Figure 13.** Structure of injection valve for two-stage rotary compressor

Figure 14 and Figure 15 show the experimental performances of different compressors. The operating frequency is 60 Hz under the ASHRAE/T condition. The cooling capacity and COP increase first and then decreases with the increase of $p_3$, and there exists a same optimum $p_3$ to maximize the capacity and COP. The reasons are as follows (as shown in figure 2): (a)when the injection pressure $p_3$ is lower, the vapor can't be completely absorbed by the 2nd stage cylinder, which makes the refrigerant (point 4) before the 2nd stage expansion valve not reach the saturated liquid state; (b) when $p_3$ is higher, the refrigerant (point 2) absorbed by the second stage cylinder contains a part of liquid, which makes the refrigerant of point 4 reach the saturated liquid state, but $h_4$ increases with the increase of $p_3$; (c) Once the suction of the secondary cylinder contains liquid, the mass flow rate of the 2nd stage cylinder will increase dramatically, then the compressor will be in the state of hydraulic compression, thus the performance will be rapidly attenuated.

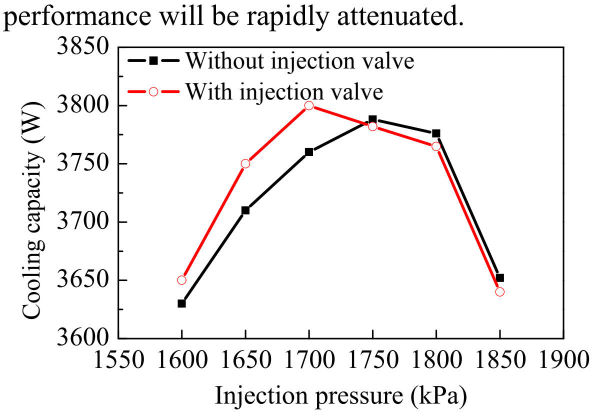


Figure 14. The cooling capacity varies with $p_3$

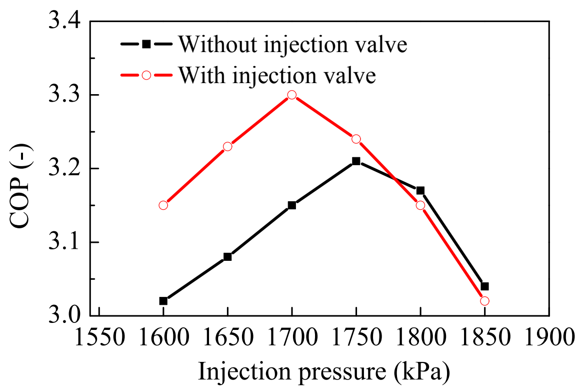


Figure 15. The COP varies with $p_3$

The optimum injection pressure is lower than that of the compressor without the injection valve, because the effective mass flow of the compressor with injection valve is increased. In addition, the influence of the injection valve on the maximal capacity is not more than 0.5%. Compared with the structure without injection valve, the optimal COP is increased by more than 2% by using injection valve. The reason is that the power loss caused by the backflow from intermediate chamber increases the power of the first stage cylinder.

## 6. Conclusions

Based on mass conservation equation, energy equation and thermodynamic identity of compressor working process, a model reflecting the refrigerant state and flow characteristics in the intermediate chamber of two-stage rotary compressor is established. P-V test shows that the simulation values of the pressure and mass flow are in good agreement with the measured values.

The simulation results show that the pressure in the intermediate chamber has obvious fluctuation characteristics. When the injection pressure is set to 1750 kPa under the ASHRAE/T condition, the peak-valley difference reaches 290 kPa, reaching 17% of the time-average value. Increasing the volume of the middle chamber can effectively reduce the pressure fluctuation and alleviate the backflow in the injection channel. The injection valve increases the amplitude of pressure fluctuation in the intermediate chamber, but the power loss of the injection is reduced by 72% ($V_4 = 2V_1$).

The validation results of the optimized prototype show that the COP of the two-stage rotary compressor with injection valve is increased by more than 2% compared with the conventional two-stage rotary compressor under the ASHRAE/T condition.

## References

[1] Building Energy Reasearch Center of Tsinghua University (THUBERC) 2016 *Annual Report on China Building Energy Efficiency* (Beijing: China Architecture & Building Press)

[2] Stefan S B and Eckhard A G 2008 Two-stage air-source heat pump for residential heating and cooling applications in northern U.S. climates *Int. J. Refrigeration* **31** 1282-92

[3] Amir A S, Alan S F and Rakesh K 2015 Performance of two-stage variable capacity air source heat pump: field performance results and TRNSYS simulation *Energy and Buildings* **94** 80–90

[4] Ma Y J, Zhang L, Fu Y, Yang X D and Jiang Y 2016 Hot-air low ambient temperature air source heat pump: a clean and efficient heating technology for farm houses in Beijing *Construction Science and Technology* **14** 76-81(in Chinese)

[5] Jin X, Wang S G, Zhang T F and Zu F 2012 Intermediate pressure of two-stage compression system under different conditions based on compressor coupling model *Int. J. Refrigeration* **35** 827-40

[6] Jiang S, Wang S G, Jin X and Yu Y 2016 Optimum compressor cylinder volume ratio for two-stage compression air source heat pump systems *Int. J. Refrigeration* http://dx.doi.org/doi: 10.1016/j.ijrefrig.2016.03.012

[7] Jiang S, Wang S G, Jin X and Yu Y 2016 The role of optimum intermediate pressure in the design of two-stage vapor compression systems: a further investigation *Int. J. Refrigeration* http://dx.doi.org/doi: 10.1016/j.ijrefrig.2016.06.024

[8] Xu S X and Ma G Y 2015 Working performance of R-32 two-stage compression system in domestic air-conditioner *Energy and Buildings* **93** 324–31

[9] Liu Q, Ma G Y and Xu S X 2013 Performance characteristics of two-stage compression heat pump system coupled with dual-cylinder rolling piston compressor *CIESC Journal* **64(10)** 3599-605(in Chinese)

[10] Redón A, Navarro-Peris E, Pitarch M, Gonzálvez-Macia J and Corberán J M 2014 Analysis and optimization of subcritical two-stage vapor injection heat pump systems *Applied Energy* **124** 231–40

[11] Zou P 2014 *Two-stage rotary compressor, air conditioner and heat pump water heater* CN Patent: 102042227B

[12] H Huang, Hu Y S, Wei H J, Yu B and Li Z P 2016 *Two-stage rotary compressor, air conditioner and heat pump water heater* CN Patent: 104110377B

[13] Ma G Y and Li H Q 2001 *Rotary Compressor* (Beijing: China Machine Press, Beijing) pp 29-40

[14] Mathison M, Braun J E and Groll E A 2008 Modeling of a two-stage rotary compressor, *HVAC & R Research* **14(5)** 719-48

[15] Shen W D, Jiang Z M and Tong J G 2001 *Engineering Thermodynamics* (Beijing: Higher Education Press) pp 33-7(in Chinese)

[16] Sieder E N and Tate G E 1936 Heat transfer and pressure drop of liquids in tubes *Industrial Engineering and Chemistry* 28 1429-35

[17] White M F 2009 *Fluid Mechanics* (New York: *The McGraw-Hill Companies, Inc.*) pp 642-52.

[18] Yu B, Wei H J and Yang O X 2019 Effect of intermediate Pressure on Performance of Single-machine Two-stage Rotary Compressor, *Journal of Refrigeration Technology* **42(1)** 43-8(in Chinese)

[19] Yin W H and Huang W C 2015 Application of PV Diagram on Refrigeration Compressor *Electrical Appliances* **7** 121-3(in Chinese)

[20] Yu B, Wei H J, Yang O X, 2018 *Two-stage enthalpy-increasing rotary compressor and air conditioner* CN Patent: 104632626B